# Changes in Fibroglandular Volume and Water Content of Breast Tissue During the Menstrual Cycle Observed by MR Imaging at 1.5 T

S.J. Graham, PhD • P.L. Stanchev, PhD • J.O.A. Lloyd-Smith • M.J. Bronskill, PhD • D.B. Plewes, PhD

**MR imaging at 1.5 T was used to investigate variations in breast parenchyma during the menstrual cycle. Seven subjects were examined twice weekly over at least one menstrual cycle. A three-point Dixon technique (TE = 19 msec, TR = 2000 msec) provided images of fat, water, and static magnetic field ($B_0$), from which two quantitative whole breast parameters were calculated: the mean relative volumetric water content, <WC>, and the mean volumetric fibroglandular fraction, <FV>. Four of seven subjects showed unequivocal cyclic variations in <WC> and <FV> consistent with expected histologic changes; <WC> and <FV> values were elevated during menses and reduced in mid-cycle. The maximum deviation measured for each of the four subjects was ≤10% in <WC> and <FV> units. These variations probably do not influence significantly the clinical interpretation of unenhanced MR breast images. Quantitative measurements of breast parenchyma, however, should recognize these effects.**

**Index terms:** MR imaging • Breast imaging • Menstrual cycle • Chemical shift imaging

**JMRI 1995**; 5:695–701

MANY WOMEN REPORT breast changes during the menstrual cycle, in particular a sense of fullness immediately before menstruation. Measurements using water displacement (1) and plaster casts (2) have shown that menstruation is accompanied by a transient increase in total breast volume. Histologic studies have also shown changes in the breast stroma and epithelium at the cellular level throughout the menstrual cycle (3,4). MR imaging provides a noninvasive, nonhazardous means of investigating changes in total breast volume, as well as macroscopic changes to the breast stroma.

Previous MR studies have produced conflicting results, which may reflect the small subject populations that have been examined to date. One study of eight subjects at 0.08 T reported detectable variations in breast volume, fibroglandular volume, and T1, that correlated with histologic studies (5). A study at 0.15 T showed changes of approximately 50% in T1 for a single subject (6). At 1.5 T, however, studies involving five subjects (7) and two subjects (8) reported no variations in proton density, T1, or T2, despite the gains in signal-to-noise ratio and spatial resolution provided by higher field strength. These prior investigations relied principally on spin-echo pulse sequences, known to provide suboptimal estimates of MR parameters (9). To provide a more accurate means of quantifying small changes in breast parenchyma, we used the three-point Dixon imaging sequence (10) at 1.5 T to differentiate adipose from fibroglandular breast tissue, and to investigate variations in breast volume and water content during the menstrual cycle. The accuracy and reproducibility of the method have been confirmed in phantoms and subjects.

## • MATERIALS AND METHODS

### *Measurement and Analysis*

Experiments were performed using a 1.5-T MR imager (Signa, General Electric Medical Systems, Waukesha, WI). Subjects were examined lying prone with both breasts suspended in a single-turn, elliptical receiver coil. The standard body coil was used for excitation. Coronal slices of 5-mm thickness and 2.5-mm separation were acquired, resulting in bilateral breast images encompassing the volume of both breasts. Analysis was performed only on images anterior to the chest wall, and therefore axillary breast tissue was not included.

From the Department of Medical Biophysics, University of Toronto, Sunnybrook Health Science Centre, 2075 Bayview Ave, Toronto, Ontario, Canada M4N 3M5 (S.J.G., P.L.S., J.O.A.L-S., M.J.B., D.B.P.). Presented at the second annual meeting of the Society of Magnetic Resonance, 1994. Received November 28, 1994; revision requested February 2, 1995; revision received March 3; accepted March 16. Supported by GE Medical Systems Canada and a Terry Fox Programme Project grant from the National Cancer Institute of Canada. **Address reprint requests to** S.J.G.

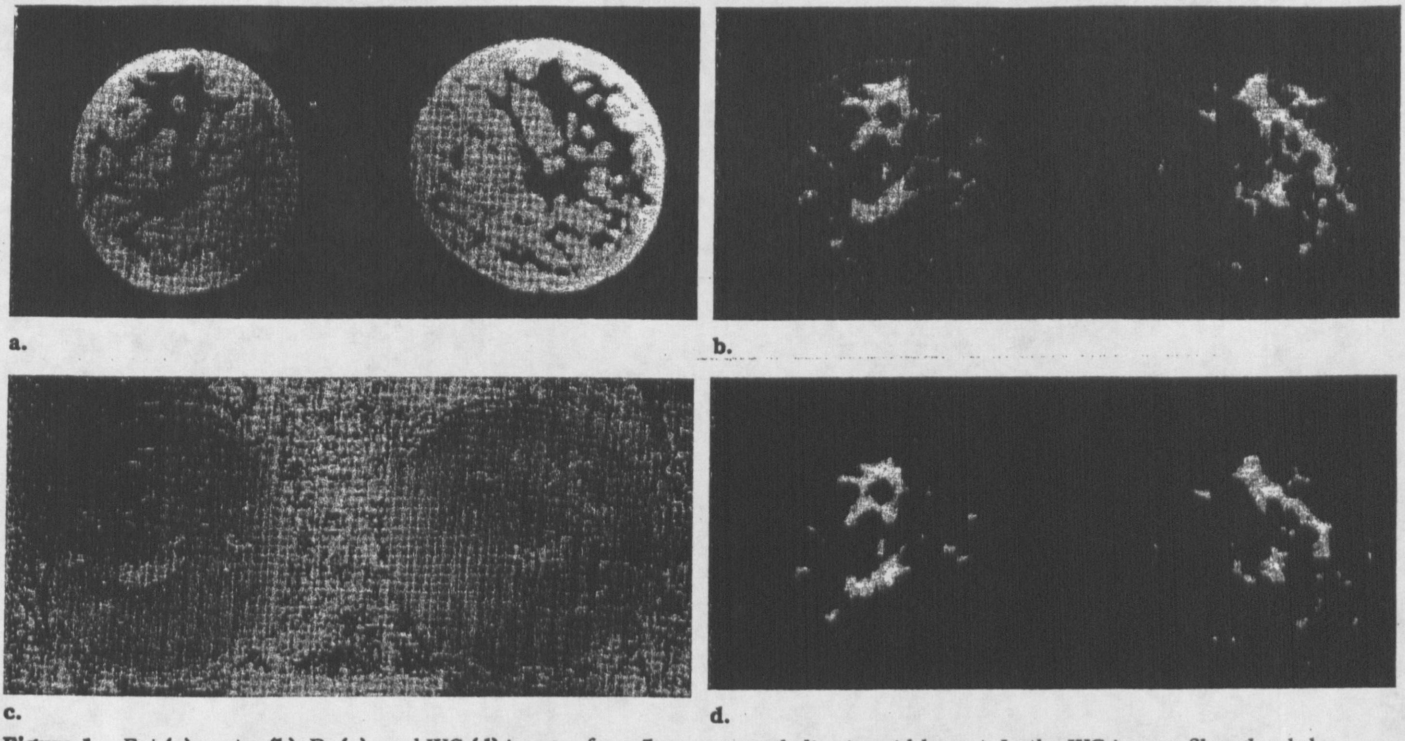

**Figure 1.** Fat **(a)**, water **(b)**, $B_0$ **(c)**, and WC **(d)** images for a 5-mm coronal slice in mid-breast. In the WC image, fibroglandular tissue appears bright.

The three-point Dixon imaging sequence (10) was used to obtain images of fat, water, and $B_0$, with TE = 19 msec and TR = 2000 msec, an acquisition matrix of 256 × 128, and a nominal field of view of 28 cm. Total imaging time was typically 13 min and examples of the images obtained are shown in Figure 1a, 1b, and 1c, respectively. The sequence also provided a standard spin-echo image (not shown). For the processed images, any signal outside the breasts, mainly noise with a little motion ghosting, was removed using a masking matrix obtained with an intensity threshold on the spin-echo image. The processed fat and water images were then used to obtain images of relative volumetric water content (WC) with the relationship

$$WC_{ij} = \frac{0.9 \cdot W_{ij}}{0.9 \cdot W_{ij} + F_{ij}} \times 100\%, \qquad (1)$$

where $W_{ij}$ and $F_{ij}$ are the signal intensities from the water and fat images at pixel location (i,j). The factor 0.9 accounts for the relative difference in proton density between water molecules and triglyceride molecules in adipose tissue, and is required to convert Equation (1) from a simple signal fraction to the volume fraction of tissue water (11). An example of a WC image is shown in Figure 1d. The normalization provided by the water content calculation effectively frees WC images from the signal nonuniformity present in water and fat images due to the receiver coil (Fig 1a and 1b), and ensures that differences in patient positioning are eliminated as a source of error in this time-course study.

The three-point Dixon sequence is susceptible to reconstruction artifacts caused by the automatic phase-unwrapping algorithm that generates the $B_0$ image (10). These artifacts typically appear as regions of abnormally high or low signal intensity compared with regions where $B_0$ has been calculated correctly, and correspond to phase errors that are multiples of $2\pi$. In regions with phase offset errors, the fat signal intensity is assigned to the water image, and vice versa. For coronal breast images this artifact can easily be corrected semiautomatically. An observer identified regions containing the phase offset artifact by thresholding the $B_0$ image, and signal intensities in the fat and water images were swapped within this region by using image processing software (Analyze, v7.0, Biomedical Imaging Resource, Mayo Foundation, Rochester, NY). Examples of this artifact for fat, water, $B_0$, and WC images are shown in Figure 2a, 2b, 2c, and 2d, respectively. The corrected WC image is shown in Figure 2e, indicating that the artifact is almost completely eliminated, and at most only a few pixels are misclassified.

The mean relative water content, <WC>, was calculated by averaging WC for all pixels in each slice for the left, the right, and both breasts. Tissue volume estimates were obtained from the pixel histogram of water content images, H(WC), and an example for the total volume of both breasts is shown in Figure 3. The minimum water content value, $WC_{min}$, is typically approximately 10%, whereas the maximum water content value, $WC_{max}$, is 100%. The histogram exhibits a large-amplitude, narrow component at approximately 15% water-content, characteristic of adipose tissue, and a low-amplitude, much broader component at higher water contents, characteristic of fibroglandular tissue. The two components blend because individual pixels can contain both types of tissue. The fractions of each type of tissue can be estimated, however, by assigning a threshold, $WC_t$, indicated by the dashed line, midway between adipose tissue and 100% water. The $WC_t$ value was chosen as 60% for all subjects. The relative volume of fibroglandular tissue was calculated as the area under the histogram to the right of the threshold, divided by the total area of the histogram, expressed as a percentage,

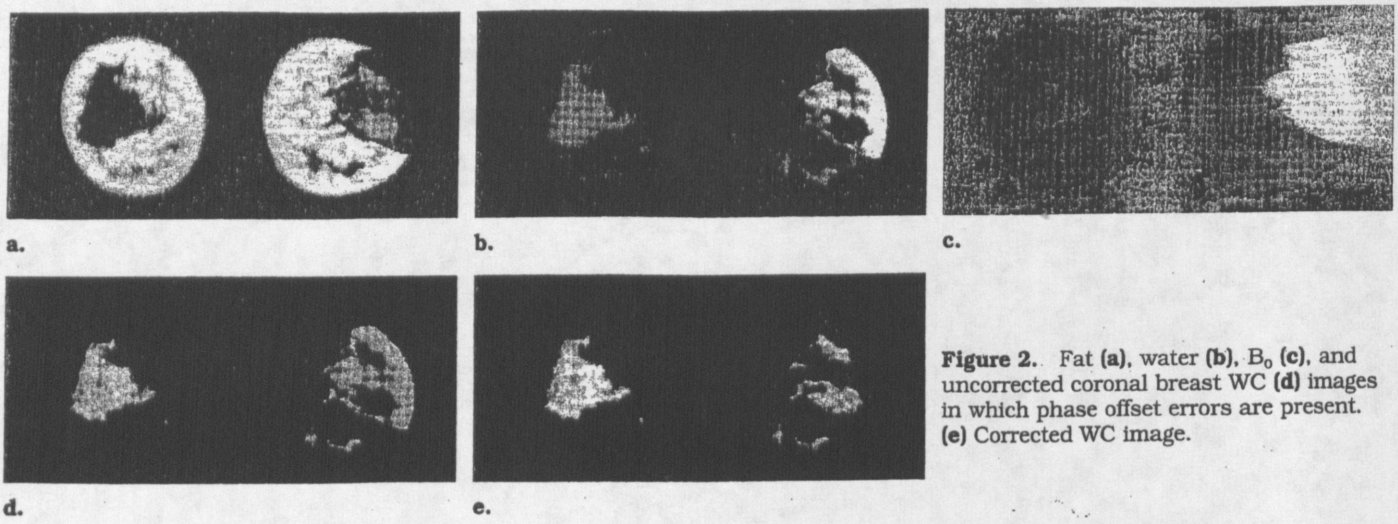

**Figure 2.** Fat **(a)**, water **(b)**, $B_0$ **(c)**, and uncorrected coronal breast WC **(d)** images in which phase offset errors are present. **(e)** Corrected WC image.

$$\langle FV \rangle = \frac{\sum_{i=t}^{i_{max}} H(WC_i)}{\sum_{i=t_{min}}^{i_{max}} H(WC_i)} \times 100\%, \qquad (2)$$

where $i_{min}$ and $i_{max}$ represent the minimum and maximum bounds on the histogram, and t corresponds to the threshold $WC_t$. Fibroglandular tissue, adipose tissue, and total breast tissue volume were also calculated for the left, the right, and both breasts.

### *Validation*

To assess the accuracy of water content and volumetric estimates, we performed two experiments with phantoms. The first experiment investigated possible errors in calculation of intravoxel water content due to the overlap of MR spectra of fat and water in 1.5-T images. While the principal spectral components of fat exhibit a chemical shift of ~3.4 ppm from the water resonance, approximately 10% of fat protons in human adipose tissue are obscured by water (12), in particular those associated with alkene bonds in unsaturated triglycerides, and alkyl glyceride bonds in all triglycerides (13). This "spectral overlap" of fat and water spectra cannot be distinguished by the three-point Dixon method, and causes overestimation of the water signal. While mineral oil contains only saturated bonds, and is thus spectrally separable from water, the fatty acid content of olive oil is ~85% by weight oleic acid, which is monounsaturated and represents a realistic estimate of the systematic error introduced by spectral overlap. In comparison, human adipose tissue contains primarily oleic acid and polyunsaturated linoleic acid, contributing 45% and 10% by weight of total fatty acids, respectively (14).

Vials of known volumetric water content ranging from 0% to 100% were prepared by mixing an aqueous solution of 0.175 mM $MnCl_2$ (T2 ≅ 80 msec) with mineral or olive oil using ultrasonification. An emulsifier, TWEEN 80 (polyoxyethylenesorbitan monooleate), was added equal to 2% of the oil volume in each vial to reduce the tendency of the mixtures to separate. No measurable MR signal was observed from TWEEN 80 itself. Water content was then measured with the MR method and compared with the known values.

To assess the accuracy of MR volume measurements when fat and water are spatially segregated, we prepared two phantoms that simulated the adipose and fibroglandular compartments of breast tissue. Each phantom consisted of a plastic bag, containing 0.175 mM $MnCl_2$, that was immersed in a bottle of olive oil. The two phantoms differed both in total volume (800 mL and 1000 mL, respectively) and in water volume (30% and 40%, respectively). The two phantoms were imaged three times using the MR protocol, with repositioning and readjustment of rf amplitude and amplifier gain settings between each set of measurements, and the mean and peak-to-peak deviations of volume estimates were assessed.

### *Subjects*

The study group included seven women, 23–37 years old, who menstruated regularly. None had used oral contraceptives or other synthetic hormones during the 6 months prior to the start of the study, and six were nulliparous. One subject had previous breast reduction surgery on one breast. For each subject, MR examinations were performed twice each week until the completion of at least one menstrual cycle. Water content and tissue volume parameters were calculated for each examination. For each subject, reproducibility was assessed in one examination by performing three repeated measurements in succession, including repositioning and readjustment of pulse amplitudes and amplifier gain settings. Anthropometric parameters such as bilateral breast symmetry, and correlation of mean relative water content with mean relative fibroglandular volume, were investigated as internal controls and to ensure that the subject sample population was representative. Correlations were assessed using the Pearson correlation coefficient, $r$, and rejecting the null hypothesis that $r = 0$ (15). Each parameter was also assessed as a function of time during the menstrual cycle.

## • RESULTS

### *Measurement Accuracy in Phantoms*

The plot of <WC> versus known volumetric water content for mineral and olive oil is shown in Figure 4. The line of identity in the graph is solid. Data points for mineral oil with true volumetric water contents of 10% and 20% are not shown because of the inability to achieve a stable emulsion. An absolute error of less than 5% in <WC> values for mineral oil mixtures is achieved over

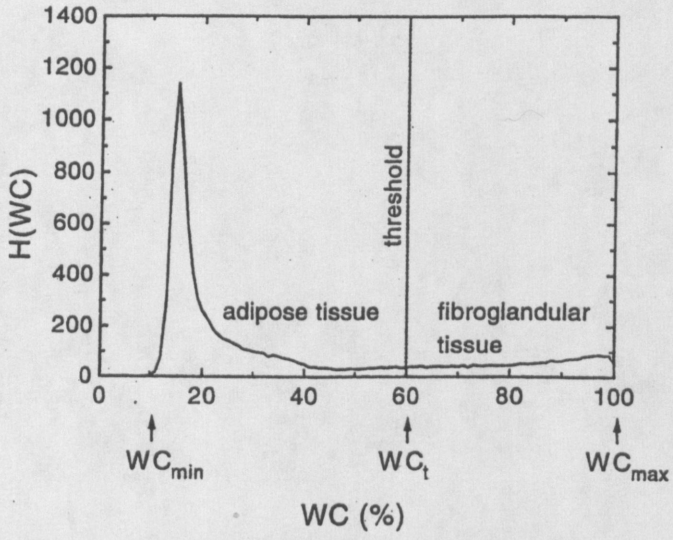


**Figure 3.** Plot of H(WC), the pixel histogram of water content for an entire breast volume. Adipose and fibroglandular tissue can be separated by the threshold indicated.

the entire range of water content, and a similar error is obtained for olive oil for water content greater than 25%. Below 25%, <WC> for the water/olive oil mixture exhibits the expected systematic error due to spectral overlap. At zero water content, the offset is 10.5%. In comparison, the stoichiometric fraction of protons in olive oil responsible for spectral overlap can be determined on the basis of the bonds in triglyceride molecules known to have the appropriate chemical shift (13), and by averaging over the different fatty acid constituents in olive oil according to their weight proportions (14). This fraction was calculated as 10%. When 10% of the total olive oil signal is taken as the "water" signal intensity in Equation (1), and the remaining 90% is taken as the fat signal intensity, <WC> is calculated as 9% and is in good agreement with observation. Above zero water content, the offset in <WC> then lessens as the true water content increases.

In Table 1, the measured volumes of phantoms are compared with the true compartmental volumes. The deviation (maximum minus minimum value) of three repeated measurements is shown in brackets in each case. The accuracy of the measurements is better than their precision. For both phantoms, the mean estimated total volume differed by less than 3%, and the mean estimated percent water volume differed by 5% or less from the expected values, whereas the deviation in estimated total volume was 0.3% or less of the mean, and the deviation in percent water volume was 1.0% or less of the mean.

### *Subject Measurements*

The mean MR parameters and peak-to-peak deviations measured for each subject are shown in Table 2. In contrast to the data in Table 1, the maximum minus minimum deviations now combine experimental error and temporal variations in the breast parenchyma. Subjects exhibited a wide range in mean breast volume, from 55 $cm^3$ to 1943 $cm^3$. Wide ranges in <FV> (3–43%) and <WC> (17–53%) values were also found, and are typical of the established, wide variation in breast parenchyma characteristics that are seen by breast radiography. Figure 5a shows a correlation plot of left versus right breast <WC> values, where the strong correlation ($r$ = .98) illustrates the strong bilateral symmetry

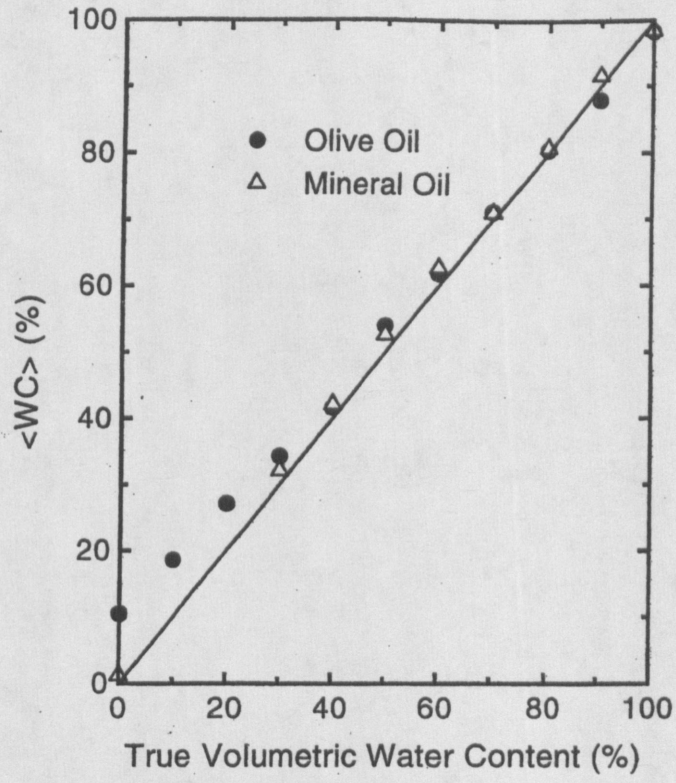


**Figure 4.** Calibration curve of <WC> versus true volumetric water content for mineral and olive oil. The line of identity is solid.

**Table 1**
**True and Measured MR Parameters for Two Breast Phantoms**

| Phantom | Total Volume ($cm^3$) | Water Volume (%) | Measured Total Volume ($cm^3$) | Measured <FV> (%) |
|---|---|---|---|---|
| 1 | 800 | 40 | 799 (2) | 38.0 (0.3) |
| 2 | 1000 | 30 | 977 (3) | 29.2 (0.3) |

Note.—The deviation (maximum minus minimum value) of three measurements is shown in brackets.

of normal breast tissue. For these subject data, a correlation of $r$ greater than .87 implies rejection of the null hypothesis that $r = 0$ with greater than 99% confidence (15). As expected, a strong correlation between mean <WC> and mean <FV> values for both breasts was also found ($r$ = .99), shown in Figure 5b. Weaker, but significant, negative correlations were found for mean <WC> and mean breast volume values ($r = -.93$) and for mean <FV> and mean breast volume values ($r = -.90$) (data not shown). These correlations are less intuitive, but agree with studies indicating that women with large volume fractions of fibroglandular tissue are on average lighter than women with breasts comprised primarily of adipose tissue (16).

To assess the temporal characteristics of the measured MR parameters, <WC>, <FV>, total breast volume, adipose tissue volume, and fibroglandular tissue volume were plotted versus time. Results for subject 2 are shown in Figure 6. The vertical axes have been expanded to illustrate the full range of variations, and the horizontal scales have been shifted to place the initial onset of menstruation at day 1. For this subject, <WC> and <FV> values clearly show menstrual changes. The absolute volume measurements, however, exhibit more scatter and do not show the expected variations.

**Table 2**
**Measured MR Parameters for Seven Subjects**

| Subject | Total Volume ($cm^3$) | Right <FV> (%) | Left <FV> (%) | Mean <FV> (%) | Right <WC> (%) | Left <WC> (%) | Mean <WC> (%) |
|---|---|---|---|---|---|---|---|
| 1 | 1944 (340) | 5.1 (1.7) | 8.0 (1.2) | 6.6 (1.5) | 19.8 (2.3) | 21.6 (1.9) | 20.7 (2.0) |
| 2 | 89 (194) | 25.7 (6.6) | 24.0 (5.6) | 24.9 (6.1) | 35.4 (5.2) | 33.8 (4.7) | 34.6 (5.0) |
| 3 | 55 (57) | 29.4 (13.0) | 35.1 (40.3) | 32.3 (21.5) | 46.4 (8.9) | 49.0 (25.3) | 47.7 (13.9) |
| 4 | 1520 (427) | 4.2 (3.7) | 2.0 (2.3) | 3.1 (2.8) | 18.6 (5.1) | 16.0 (3.3) | 17.4 (4.0) |
| 5 | 592 (220) | 30.9 (10.4) | 24.2 (11.8) | 27.7 (11.1) | 39.6 (8.5) | 34.6 (9.4) | 37.2 (9.0) |
| 6 | 181 (89) | 41.7 (8.8) | 44.7 (6.52) | 43.3 (5.2) | 51.7 (6.7) | 53.7 (4.8) | 52.8 (4.5) |
| 7 | 830 (255) | 5.1 (1.7) | 8.0 (1.2) | 6.6 (1.5) | 19.8 (2.25) | 21.6 (1.9) | 20.7 (2.0) |

Data for all seven subjects were summarized by plotting <WC> for the total volume of both breasts as a function of time (Fig 7). Error bars indicate the maximum and minimum values of three repeated measurements during one examination for each subject. When compared against experimental error, subjects 1, 2, 4, and 5 show unequivocal cyclic variations (i.e., increased <WC> within 4 days of the onset of menses and decreased <WC> in mid-cycle). Subject 7, who had a regular menstrual cycle for the prior 6 months, experienced short, irregular menstrual cycles during the study, which contributed additional variability. For the two subjects with the smallest breast volumes (subjects 3 and 6), the expected cyclic variations were not detected.

## • DISCUSSION

The results with phantoms indicate that the measurements of <WC> and <FV> are quite accurate and precise in determining relative volumetric water content and fractional fibroglandular volume. The systematic offset at low <WC> values due to the overlap of water and fat spectra is less than 10% water content and primarily affects estimates of water content in adipose tissue. The arbitrary positioning of the threshold $WC_t$ to separate adipose from fibroglandular tissue in the water content histograms (see Fig 3) also causes a small systematic error in <FV> values. In both cases, however, these errors affect absolute accuracy but have little impact on the ability to detect temporal changes in breast parenchyma.

The broader experimental deviations observed for subject data in Table 2 and the time course data in Figure 7 indicate that small changes in breast tissue due to cyclic variations in female hormones can be detected with MR imaging at 1.5 T. The observed changes are qualitatively consistent with prior histologic investigations that support the observation of transient increases in water content and fibroglandular volume at or near the time of menstruation (3,4). The maximum cyclic variations seen were approximately 10% water content and 10% fibroglandular volume for subject 5, but are unlikely to impact the clinical interpretation of unenhanced MR breast images. The effects of the menstrual cycle on contrast-enhanced MR breast imaging cannot be assessed directly from this study.

Measurements of total breast volume and adipose tissue volume with our methodology did not exhibit the expected menstrual variations (see Fig 6). On biological grounds, the adipose tissue volume should remain constant because the requisite hormone receptors are absent, and the total breast volume and fibroglandular volume should track with <FV>. Instead, the total breast volume and adipose tissue volume show similar variations that are anticorrelated with <WC>, <FV>, and fibroglandular volume. The volume measurements were strongly influenced, however, by the number of slices used in the calculations. The slice closest to the chest wall was included or excluded due to partial volume considerations, depending on subject positioning from examination to examination, and made major contributions to the total breast volume and adipose tissue volume estimates. Smaller errors were introduced by minor rotations of the patient about the axis of the magnet bore. The use of a 2.5-mm gap between slices may also have affected the reproducibility of absolute volume estimates, although this effect is likely to be minor in most cases.

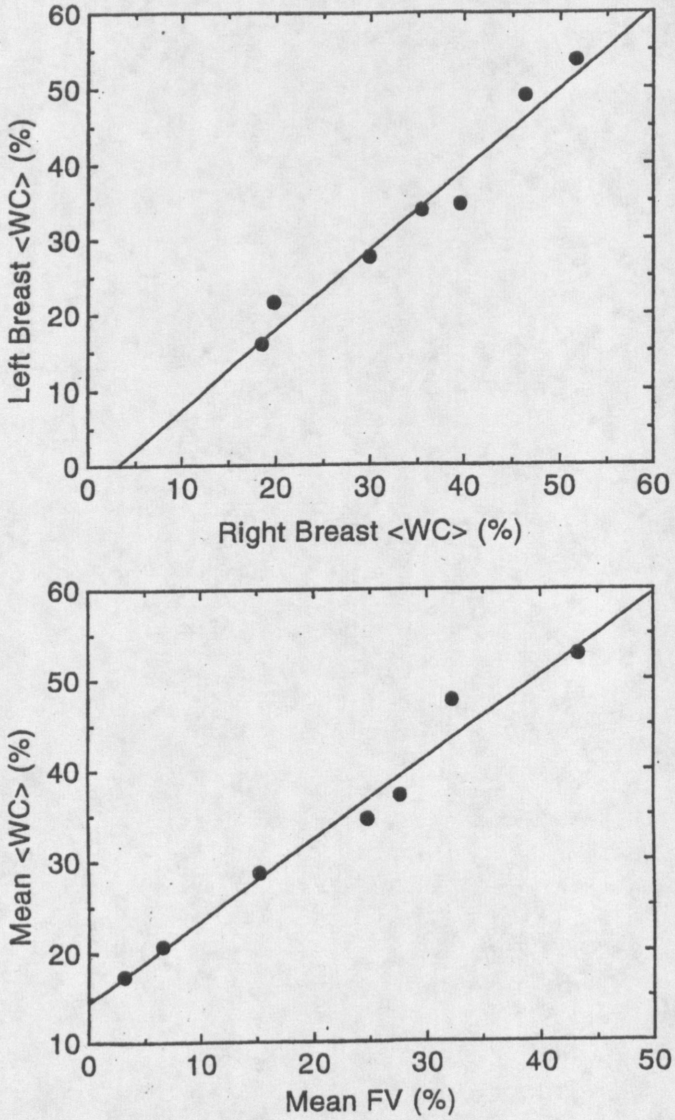


**Figure 5.** Correlation plots of **(a)** left versus right breast <WC> and **(b)** mean <WC> versus mean <FV> values. Linear regression line is solid.

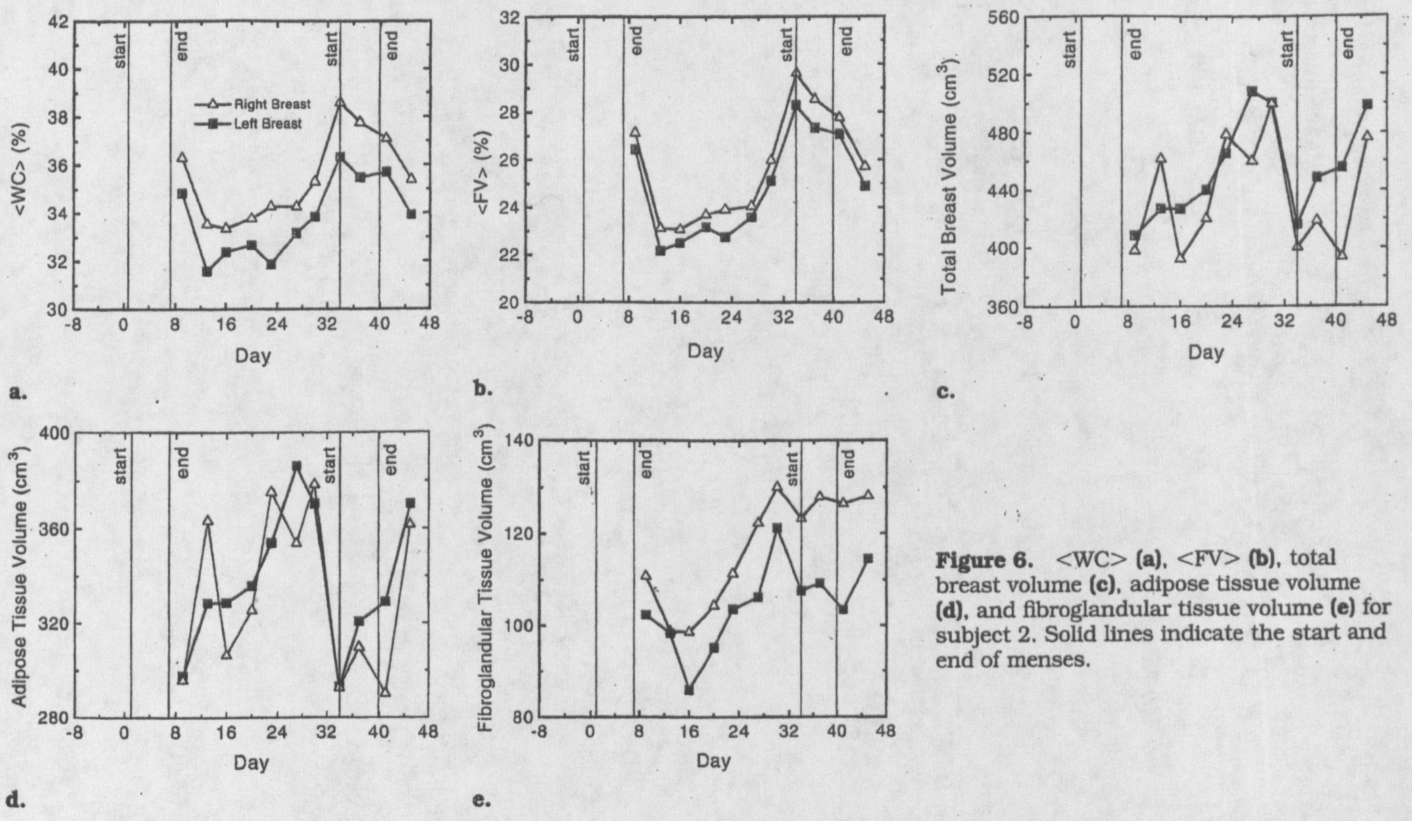


**Figure 6.** <WC> **(a)**, <FV> **(b)**, total breast volume **(c)**, adipose tissue volume **(d)**, and fibroglandular tissue volume **(e)** for subject 2. Solid lines indicate the start and end of menses.

Measurements have indicated that except in the region close to the nipple, the relative water content and fibroglandular fraction vary only slowly from slice to slice (data not shown).

Calculation of <FV> and <WC> as relative quantities reduced the effects of these factors greatly. For the five subjects with largest total breast volume, the inclusion or exclusion of the slice nearest the chest wall made no more than a 2% absolute difference in the calculated value of <WC> or <FV>. For the two subjects with small total breast volume, the difference was larger, but less than 5%. Thus, these two parameters provide the clearest indications of menstrual cycle effects. The fibroglandular tissue volume, mainly located anterior to the retromammary fat layer, was also less sensitive to the total number of slices included.

The results of this study are qualitatively similar to those of Fowler et al (5) at 0.08 T, who pooled and normalized data from eight women measured at sparse time intervals to encompass four to eight consecutive menstrual cycles. They found mean variations of 13%, 39%, 15%, and 25%, in breast volume, fibroglandular volume, fibroglandular T1, and fibroglandular tissue water content, respectively, although measurements of individual subjects differed widely. These mean variations are somewhat larger than obtained in our study at 1.5 T, and probably reflect the different normalization strategies of the two studies. Whereas the data of Fowler et al were normalized to the values during menses for each subject, our <WC> and <FV> values were normalized by volume. The detailed data from our study, measured over one menstrual cycle, suggest that the magnitude of <WC> and <FV> variations is usually small. This can explain why previous studies of smaller subject populations at 1.5 T failed to detect changes (7,8).

There are, nevertheless, some applications of quantitative MR breast imaging in breast cancer etiology and epidemiology in which small tissue changes during the menstrual cycle should be recognized. There is indirect evidence that large <WC> and <FV> values are risk factors for breast cancer (17) and quantitative analysis of breast radiographs shows clearly that the pattern of the breast parenchyma is a major risk factor for breast cancer (18). Case-control studies investigating these relationships could be enhanced by performing all measurements at the same phase of the menstrual cycle. Menstrual cycle effects could also influence identification of the subset of women at highest risk, investigation of the reduction in fibroglandular components of the breast with age, and monitorship of the effect of hormonal therapy for reducing breast cancer risk (19).

We conclude that variations in breast tissue characteristics during the menstrual cycle are detectible at 1.5 T in some subjects by using the three-point Dixon imaging sequence. The variation in breast water content and fibroglandular volume correlates qualitatively with the known effects of hormones on breast structures. These variations are small and unlikely to impact clinical assessment of unenhanced MR breast images, but quantitative measurements of breast parenchymal patterns should recognize these effects.

**Acknowledgments:** The authors thank Erika Schneider for assistance in this study, and Pauline Houston, David Johnstone, and Julie Sherwood for imaging the subjects.

## References

1. Milligan D, Drife JO, Short RV. Changes in breast volume during normal menstrual cycle and after oral contraceptives. Br Med J 1975; 4:494–496.
2. Ingleby H. Changes in breast volume in a group of normal young women. Bull Int Assoc Med Mus 1949; 29:87–92.
3. Longacre TA, Bartow SA. A correlative morphologic study of human breast and endometrium in the menstrual cycle. Am J Surg Pathol 1986; 10:382–393.
4. Vogel PM, Georgiade NG, Fetter BF, Vogel FS, McCarty KS. The correlation of histologic changes in the human breast with the menstrual cycle. Am J Pathol 1981; 104:23–34.

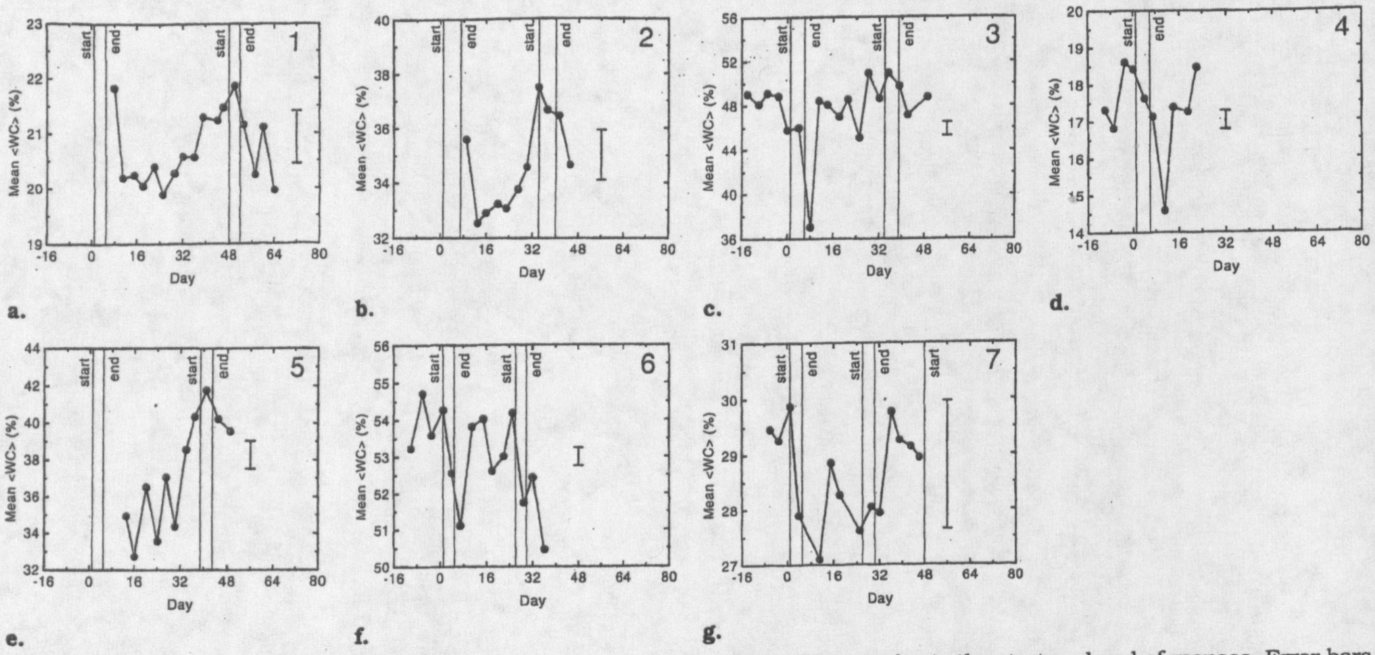


**Figure 7.** Plots of mean <WC> versus time for seven subjects **(a)–(g)**. Solid lines indicate the start and end of menses. Error bars for each subject represent the deviation (maximum minus minimum value) of three repeated measurements during one examination. Different mean <WC> scales are used to show the full range of variations for each subject.


5. Fowler PA, Casey CE, Cameron GG, Foster MA, Knight CH. Cyclic changes in composition and volume of the breast during the menstrual cycle, measured by magnetic resonance imaging. Br J Obstet Gynaecol 1990; 97:595–602.
6. Nelson TR, Pretorius DH, Schiffer LM. Menstrual variation of normal breast NMR relaxation parameters. J Comput Assist Tomogr 1986; 9:875–879.
7. Martin B, El Yousef SJ. Transverse relaxation time values in MR imaging of normal breast during menstrual cycle. J Comput Assist Tomogr 1986; 10:924–927.
8. Jawny LM, Wicks A, Hornak JP, Totterman SM. Breast tissue T1, T2, and rho values during the menstrual cycle (abstr). In: Proceedings of the Society of Magnetic Resonance in Medicine, 1993. New York: Society of Magnetic Resonance in Medicine, 1993; 858.
9. Poon CS, Henkelman RM. Practical T2 quantitation for clinical applications. J Magn Reson Imaging 1992; 2:541–553.
10. Glover GH, Schneider E. Three-point Dixon technique for true water/fat decomposition with $B_0$ inhomogeneity correction. Magn Reson Med 1991; 18:371– 383.
11. Poon CS, Szumowski J, Plewes DB, Ashby P, Henkelman RM. Fat/water quantitation and differential relaxation time measurement using chemical shift imaging technique. Magn Reson Imaging 1989; 7:369–382.
12. Mao J, Yan H, Brey WW, Bidgood WD Jr, Steinbach JJ, Mancuso A. Fat tissue and fat suppression. Magn Reson Imaging 1993; 11:385–393.
13. Chapman D, Goñi FM. Nuclear magnetic resonance spectra. In: Gunstone FD, Harwood JL, Padley FB, eds. The lipid handbook. London: Chapman and Hall, 1986.
14. Weast RC, Astle MJA, Beyer WH, eds. CRC handbook of chemistry and physics, 64th ed. Boca Raton, FL: CRC Press, 1984; D-221.
15. Hays WL, Winkler RL. Statistics: probability, inference, and decision. New York: Holt, Reinhart & Winston, 1971.
16. Brisson J, Morrison AS, Kopans DB, et al. Height and weight, mammographic features of breast tissue and breast cancer risk. Am J Epidemiol 1984; 119:371–381.
17. Poon CS, Bronskill MJ, Henkelman RM, Boyd NF. Quantitative magnetic resonance imaging parameters and their relationship to mammographic pattern. J Natl Cancer Inst 1992; 84:777–780.
18. Warner E, Lockwood G, Tritchler D, Boyd NF. The risk of breast cancer associated with mammographic parenchymal patterns: a meta-analysis of the published literature to examine the effect of method of classification. Cancer Detect Prev 1992; 16:67–72.
19. Spicer DV, Ursin G, Parisky YR, et al. Changes in mammographic densities induced by a hormonal contraceptive designed to reduce breast cancer risk. J Natl Cancer Inst 1994; 86:431–436.

(44.) * Graham S., Stanchev P., Lloyd-Smith J., Bronskill M., Plewes D., "Changes in Dibroglandular Volume and Water Content of Breast Tissue During the Menstrual Cycle Observed by MR Imaging at 1.5 T", ***JMRI*** No. 5, 1995, 695-701.